Forming Behavior and the Structure of Glasses

Alexis G. Clare, Wesley A. King and William C. LaCourse
New York State College of Ceramics at Alfred University, Alfred, NY

Abstract

The effect of forming on arsenic selenide glass fiber drawn under extreme conditions are discussed in detail. Differential Scanning Calorimetry (DSC) data are correlated with previously published time-of-flight (TOF) neutron scattering, nuclear quadrupole resonance (NQR) data to argue that the structure of As_2Se_3 glass pulled under extreme conditions is oriented and that some of the extreme structures imposed in the arsenic selenide fibers relax at room temperature. A model is proposed for the sequence of events suggesting a regime of interchain breakage followed by reformation followed by intrachain breakage. Also evident are unexpected small ring structures as a result of low temperature healing process.

I. Introduction

The existence of structural orientation in glass fiber is still a topic very much in dispute by a rather large number of people. Experiments performed by Stockhorst and Brückner show that glasses with a lower dimensionality exhibit a greater tendency towards draw-induced structural anisotropy than more three-dimensional glasses.[1-4] These workers showed that structural orientation influences the optical properties of these fibers. It is believed that extreme forming conditions can lead to unsatisfied bonding via partial fracture which is linked to "shear thinning", a non-Newtonian decrease in viscosity that occurs with increasing shear rates [5]. If the forming temperature is too low, or the forming rate too high, relaxation of the structure is unable to offset the rapid bond rearrangements and intermediate metastable structural arrangement may result. Studies on silicate glasses [6] and some other work on chalcogenide glass fibers [7] are suggestive of such rearrangements.

Previous evidence of anisotropy in fibers due to extreme forming have been inferred by observations of anisotropy in the mechanical and thermal properties [8-17]. X-ray diffraction investigations of B_2O_3 glass fibers [18] also indicated orientation in the structure which enhanced on aging. Later investigations [19] on borate and phosphate glass fibers agreed, but all results were disputed [20] on the grounds that hygroscopicity of the materials may have been responsible for some of the observations. Alkali metaphosphate fibers were reported to exhibit structural orientation in two studies [21-22] using X-ray diffraction. These studies along with those of Stockhorst and Bruckner, imply that chain-like structures are more liable to orient, whereas no observable orientation occurred in more three-dimensional examples, such as E-glass [23].

If anisotropy is induced in a glass upon forming, a change in the fictive temperature of the glass would be expected. In addition, if these structures are metastable structures resulting from shear thinning, a relatively low temperature relaxation of these structures might be observed. Indeed sub-T_g relaxation has been observed in a number of glass systems including oxides [6, 24], halides [25], chalcohalides [26] and chalcogenides [27]. One of the ways in which this relaxation manifests itself is in pre-T_g exotherms, where a release of stored energy is observed.

The occurrence of relaxation phenomena at temperatures well below T_g for glass fibers, even those with silicate compositions, is not an exclusive indication of structural orientation, since rapid cooling during fiber drawing results in a higher fictive temperature structure. A fiber will generally possess a lower effective viscosity in relation to the bulk glass, resulting in a decreased barrier to structural rearrangement. The formation of defects, such as broken bonds or high energy bonding arrangements, also plays a role in low temperature relaxation behavior for glass fibers. This was seen in some differential scanning calorimeter (DSC) data for rapidly-drawn silicate fibers [6].

The sub-T_g relaxation of As-Se glass fibers was examined by Sheih [28] and Sheih and LaCourse [12], who observed changes in the fiber mechanical properties with aging and annealing. Bending strength decreased as a function of aging time at ambient temperature, with the selenium rich fibers showing the greatest decrease in strength, whereas, the elastic modulus of the fibers was observed to increase with room temperature aging. The room temperature relaxation [12] of stress at constant

strain for fibers was explained in terms of the fibers displaying a broad distribution of relaxation times, including rapid, low temperature relaxations. Extensive DSC measurements on arsenic selenide glass fibers and pressed samples were made by Cerqua-Richardson [7], who examined the stored energy in a variety of As-Se samples as a function of aging and forming conditions. The stored energy was determined by integrating the difference between the initial DSC spectrum, containing the exothermic feature, and that of a well-annealed sample of the same composition. A slightly modified method was used by Ho [6] to measure the energy stored in silicate fibers during the drawing process. Cerqua-Richardson reported that the dependence of the measured stored energy on aging and forming conditions showed a complex behavior. The exotherm area for two As_2Se_3 fiber samples drawn at slow rates first decreased with aging at sub-T_g temperatures (room temperature and 75° C) but then increased with further aging. The initial decrease was larger for the samples aged at 75° C. A similar dependence on draw speed was observed for the bend strength data reported by Sheih [28]. The electron paramagnetic resonance work done by Cerqua-Richardson shows that the production of structural defects is dependent upon the draw rate in a way almost identical with the stored energy. The density of electron spins, which is reflective of structural damage in the fibers, supports the idea of shear thinning during fiber drawing.

Rather more conclusive evidence of draw-induced structural orientation in arsenic selenide glass fibers drawn under more extreme conditions than previous studies has been presented through neutron scattering and NQR experiments [29,30]. This evidence is summarized and correlated to the thermal analysis data in which relaxation of metastable structures formed as a result of these conditions will be demonstrated. These experiments also show that at certain shear rates, healing mechanisms become operative for which a structural model is proposed.

II. Experimental Procedure

1-5 mm long fiber pieces up to 25-50mg were hermetically sealed into aluminum pans and placed into the DSC for measurement. The enthalpy of arsenic selenide glass fiber samples was measured using a Mettler heat-flux Model DSC30 [Mettler Thermal Systems, Greifensee, Switzerland] DSC instrument. All fiber samples tested in the "fresh" condition were stored in liquid nitrogen (LN_2)

immediately after drawing until just prior to the DSC measurements. Aged fiber samples were held in a small furnace at 303 K for various times, or the aging was performed in the DSC instrument itself. Samples were heated from 293 K to 523 K at 10 K/min, cooled back to 293 K at 5 K/min, and then reheated to 523 K at 10 K/min to establish a reference curve. These cyclic heating and cooling measurements were used to first obtain the stored energy and then calculate the fictive temperature for the samples. Samples remained in the DSC during the cyclic heating schedules to maximize the measurement accuracy. Selected samples were heated through the transition region at a variety of rates to obtain information about the kinetics of the sub-T_g relaxation. Still other samples were scanned from low temperatures ($T < 273$ K) to investigate possible low temperature relaxations. Nitrogen gas was flowed through the sample chamber at 10 mL/min to purge the chamber during all measurements.

Table 1

Drawing conditions for the fiber samples examined using the DSC.

Sample	Draw Temperature (K /°C)	Draw Rate (m/min)	Argon Pressure (psi / Pa)	Fiber Diameter (±2μm)	Bulk Glass T_g (± 2 K)
A	593 / 320	66	1.25 / 8600	77	453
B	593 / 320	90	1.40 / 9600	65	453
C	593 / 320	107	1.75 / 12000	76	453
D	593 / 320	111	1.75 / 12000	70	453
E	593 / 320	127	1.80 / 12400	70	454
F	593 / 320	150	1.85 / 12700	70	453
G	593 / 320	156	2.00 / 13800	77	454
H	593 / 320	167	2.10 / 14500	65	454

The pre-T_g exotherm and glass transition onset temperatures were determined using the intercept method procedure. The exotherm areas (Joule/gram) were found by first subtracting the reheated sample signal (no pre-T_g exotherm) from the initial signal showing an exotherm, resulting in a difference spectrum. Exotherm areas were calculated by integrating this difference spectrum from temperatures well below the exotherm onset temperature to a fixed reference

temperature, which was the fictive temperature for the relaxed sample (T_f). This temperature value was calculated using an area matching technique described by Moynihan et al. [31].

The fictive temperature of each relaxed sample was obtained from the DSC trace upon reheating the sample at 10 K/min after a 5 K/min cool through the transition region. This measurement technique was used by Ho [6] and allows calculation of the sample's initial fictive temperature from the measured pre-T_g exotherm area. For each fiber sample, the baseline was constructed by connecting the tangents to the DSC curve at $T_1 << T_g$ and T_2=493 K, a temperature in the equilibrium liquid region. Baselines were usually flat, or horizontal, however, the thermal contact for the samples sometimes changed on heating past the T_g region, resulting in a shift in the DSC baseline. It has been shown that the activation energy for structural relaxation can be calculated from DSC data measured using various heating or cooling rates [31,32-34]. The relevant relationship is described by

$$\frac{d\ln|q|}{d\left(1/T_f\right)} \approx -\frac{\Delta h^*}{R} \qquad \text{Equation 1 [33]}$$

where q is the heating or cooling rate, T'_f is the limiting fictive temperature, Δh^* is the activation energy, and R is the gas constant. Using the onset glass transition temperature, T_g, instead of T'_f in the equation above, Moynihan et al. [34] reported a Δh^* value of 70 kcal/mol for As_2Se_3 glass. That value was later corrected to 81.8 kcal/mol when the fictive temperature was used in the computation [33]. Using measurements of the onset T_g, much lower values for Δh^* (≈ 50 kcal/mol) were reported by Cerqua-Richardson for As_2Se_3 bulk glass and fibers [7].

A similar method was used here to compare apparent activation energies for the sub-T_g relaxation in several samples. In these cases, the exotherm onset temperature was used instead of the fictive temperature or the glass transition temperature in Equation 1. The mathematical basis for this method is less rigorous than for the studies cited above, yet the activation energies computed can be used as comparative values. The primary assumption is that the relaxation kinetics possess an Arrhenius relationship with temperature. It is also assumed that the contribution of the differential heat capacity with respect to the reciprocal temperature is small compared to that of the relaxation time. The pre-T_g relaxation

onset temperatures were measured from the DSC enthalpy curves using the intercept method with an estimated error of ± 3 K. The results of these measurements are presented here to qualitatively compare the as-formed glass fiber structures for some samples.

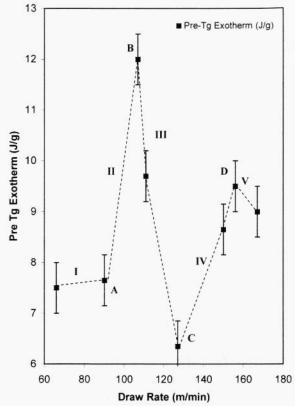

Figure 1 The effect of draw rate on the measured store energy via DSC and the effect of draw rate on onset temperature for the pre-T_g exotherm (dotted lines are a guide to the eye)

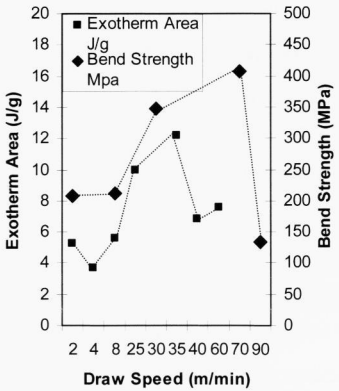

Figure 2 Exotherm area and bend strength versus draw rate for arsenic selenide fibers (from [6] and [28]) (dotted lines are a guide to the eye)

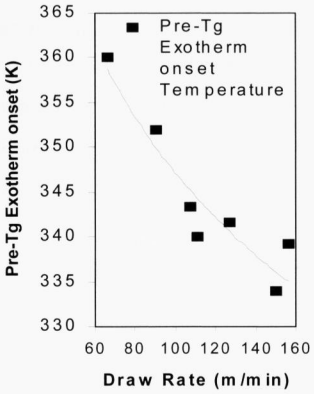

Figure 3 The effect of draw rate on the measured stored energy via DSC and the effect of draw rate on onset temperature for the pre-T_g exotherm (dotted lines are a guide to the eye)

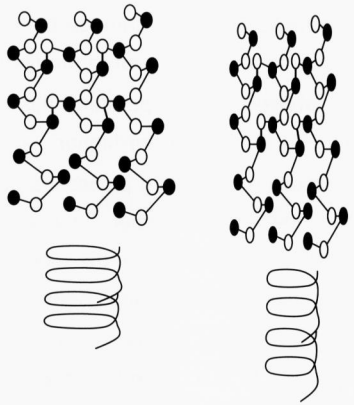

Figure 4 Schematic of the effect of stress on the structure of the glass during cooling

III. Results

Figure 1 illustrates the influence of draw rate on measured stored energy, The fictive temperature shows similar dependence. The stored energy versus draw rate shows a striking similarity to that obtained by Sheih and Cerqua-Richardson (figure 2). Figure 3 shows the Pre-T_g exotherm onset temperature as a function of draw rate.

IV. Discussion

The data in Figure 1 illustrate the influence of draw rate on the measured stored energy for rapidly-drawn fibers which, as mentioned, closely resemble those trends reported by Sheih [28] and Cerqua-Richardson [7]. Samples A-H were drawn so that the fiber diameter, and hence the approximate cooling rates, were similar (70 μm ± 5μm diameter) to reduce the variation in fictive volume-type contributions to the stored energy. Despite this method, the cooling rate would still be slightly dependent upon the drawing rate, although the effect was less than for very small fibers drawn at high temperatures, such as those investigated by Ho [6]. As the draw rate increases, the stored energy appears to build up and is then released as the rate reaches two critical thresholds. It is proposed that at higher rates, the stored

energy (measured after drawing and using a DSC) is not only a function of this draw-induced structural damage but also of rapid relaxation or healing processes that become significant before the fibers can be stored in LN_2. Since the T_g is not too far above room temperature, this rapid relaxation scenario is more reasonable for As_2Se_3 fibers than for higher T_g systems, such as silicate-based glass fibers. The relaxation or healing processes taking place must be extremely energetic and have a low kinetic barrier, otherwise, they would not be significant at room temperature. After drawing, the most energetic and mobile relaxation mechanisms could proceed some distance before being arrested by the LN_2 storage. However, as indicated by the previously published NQR data the relaxation never regresses the structure to that of the bulk glass. Fibers drawn at 107m/min show a maximum in the NQR spectrum with sharp peaks consistent with the sharp NQR lines seen for As_2Se_3 crystals although the sample was found to be X-ray amorphous [30].

As shown in Figure 3 for the fresh samples, the exotherm onset temperature generally decreases with draw rate, indicating that the spectrum of relaxation times is shifted to more rapid processes with increasing draw rate [35]. As the draw rate increases, the glass experiences a greater quench rate, thereby freezing in a higher fictive temperature and more open structure. Upon reheating, the release of excess energy can commence at lower temperatures for such fibers, owing to their greater driving force and lower kinetic barrier.

The data presented in this paper suggest that there are distinctive forming regions, where the effects of the draw-induced damage and complimentary healing process differ. A more sophisticated model is needed to describe the current results and should include details of the glass structure. As the glass is drawn into a fiber, the tensile drawing stresses tend to elongate the rings situated along the fiber axis as they are trying to cool, whereas the corresponding compressive stress tends to flatten the rings in the radial direction. The same process could also be described as a stretching of the spiral As-Se chains in the axial direction. This process is shown schematically in Figure 4. At the same time, the rapid cooling causes the bond length and angle distortions to be frozen in the structure, raising the internal energy slightly. As the drawing rate increases, the ring bonds, which also act as lateral cross-linking bonds between adjacent chains, rupture under the influence of heat and do not reform because of the increasing shear stresses. The chain structures then become more oriented as lateral bond rupture forces the intact chains to

accommodate additional stresses. In this way, the shear thinning process can rapidly approach a critical stage. At the same time, the fiber is being quenched, effectively freezing all but the most mobile defect species into the structure. Were it not for the relaxation or healing process, the energy stored in the fibers should increase up to the point where the fiber breaks through the coalescence of damaged regions.

Bonds left dangling during drawing greatly increase the energy of the structure, and fibers that can retain the broken bonds will show a larger stored energy. Regions with a high concentration of broken bonds will possess a decreased effective viscosity, and the probability of low temperature structural rearrangement increases in such regions. The chances of defect annihilation through bond reformation also increases where the concentration of defect species is high. The regions between adjacent chains would be expected to have high defect concentrations, since the shear stress is high there. Some inter-chain defects will then be eliminated, as the bonds on nearby defects reform and lower the energy of the structure.

At very high rates and stresses, dangling bonds are formed not only from the lateral, inter-chain bonds, but now some of the intra-chain bonds are broken. The newly-formed chain ends will snap apart, since the chain is under a tensile load, but the separation will be arrested at some point when the broken lateral bonds reform with their opposites on the adjacent chain. These chain ends may also reform bonds with neighboring defects, but the broken chains will not heal to form oriented chains but rather will form rings or bent chains. The chances of creating empty void space in the structure are greater once the chain structures begin to snap.

The simultaneous action of the proposed mechanisms is complex, but such a scenario can satisfactorily explain both the measured exotherm data in Figure 1, which has been divided into five regions. In region I, the drawing stress is insufficient to cause many broken bonds, and so the measured stored energy is not very sensitive to the draw rate. The major contribution to the stored energy is the frozen-in strain, which was demonstrated by crushing some of the fresh Sample B fibers under LN_2 and measuring the resultant energy release. The amount of energy left in the crushed fibers was only 40% of the original fresh value. DSC measurements on aged fibers suggest that the stored strain increases with draw rate, and this also supported by neutron scattering and NQR data for fibers drawn

under similar conditions [29,30]. After the onset of shear thinning at critical point "A" in figure 1, the lateral or inter-chain bonds start to break, quickly raising the stored energy in the fibers. The defect concentration in region II is initially low, so the defects are relatively isolated and unable to cooperatively reform. After critical point "B", the defect concentration is high enough to make the structure energetically unstable, and a portion of the broken cross-link bonds reform into rings, thereby lowering the stored energy. Results from the NQR study suggest that the reformed ring structures are smaller than those in the bulk glass and similar to those found in crystalline As_2Se_3 or As_4Se_4. Such ring structures would be more stable energetically than the larger rings found in the glass, and the energy release from bond reformation would lower the stored energy. The NQR sample that gave the most crystalline-like features in the spectrum corresponds to the draw rate in which the maximum stored energy was seen in the DSC.

As the rate is increased in region III, increasingly more of the damaged regions can relax, since the rising number of broken bonds reduces the effective viscosity in those regions. At critical point "C", the stored energy is actually less than the values measured for region I fibers. This suggests that some of the frozen-in bond length and angle distortions (stored strain) are eliminated under these conditions, as more of the structure becomes involved in the rupture and heal process. The stored energy increases with draw rate again in region IV, where the energy released by the healing process cannot keep up with the structural damage incurred. Intra-chain fracture must be occurring in region IV, but it is unclear whether point "C" marks the onset of chain rupture or the increasing significance of chain rupture. In any case, the stored energy continues to increase with draw rate in region IV up to critical point "D". The only sample drawn in region V was Sample H, which did not show the same pre-T_g exothermic behavior as the other samples. Considering that the total stored energy value for Sample H is greater than 9 J/g, then point "D" cannot conclusively be labeled as a critical point. Since Sample H exhibited relaxation at much lower temperatures (200 K below T_g) than the other fiber samples, the residual damage in these fibers may be slightly different than for the other samples. Bond switching may partially explain the very low temperature relaxation, but the As-As, As-Se and Se-Se bond energies are similar, so the energy released through this mechanism would be relatively small. It is possible that similar relaxations occurred in the other fibers and happened before the sample was

measured.

As previously reported [29] the neutron scattering data clearly shows structural orientation effects in fibers drawn at a rapid rate (156m/min). A feature in the total correlation function at 5.6Å is shifted to shorter distance in the radial direction and to longer distance in the axial direction. This feature has been correlated before with distances within the As-Se chains which can be visualized in the crystal structure as cross-linked "springs" (Figure 4). When a spring is stretched, its cross-section becomes smaller and the distance between adjacent spirals larger. Hence, if chains align and stretch along the axis of the fiber draw then a decrease in radial correlation distances (spring cross-section) and an increase in axial correlation distances (distance between adjacent spirals) is expected. Even more interesting however is the origin of the 4-5Å feature seen in he total correlation function. As correlations predominate in the crystal at these distances, the appearance of this feature might imply devitrification. There is no evidence of this in larger scale in either X-ray or neutron diffraction patterns. However, if indeed shear thinning occurs during pulling, the aligned chains essentially slide over each other so fast that the cross-linking cannot occur and the structure contains many energetically unfavorable dangling bonds. These defect arrangements are high energy, and bond reformation can lead to localized crystalline arrangements, such as small rings, which are normally not seen in the glass. The important question is; at what drawing speeds can this process of defect creation and relaxation take place?

The neutron experiments were performed on fibers drawn under region I and region IV (near point D) conditions. The more slowly-drawn fibers showed little anisotropy and no significant damage to the ring structures. Results for the rapidly-drawn fibers showed that the ring structures were disrupted, and that anisotropic strains, arising from the uniaxial drawing stresses, remained frozen in the structure. In addition to these observations, a correlation distance, previously unseen in the bulk glass, appeared and was particularly evident in the axial direction. This correlation length was similar to characteristic distances for the small ring structures present in crystalline As_2Se_3 and As_4Se_4. The proposed physical model for the fiber's structural response during drawing provides a plausible explanation for these interesting experimental results.

V. Conclusions

Previously reported scattering data taken for fibers drawn at 70m/min and 156m/min show evidence of structural anisotropy in the faster drawn fibers. This is indicated by shifts in the correlation distances consistent with the structural conception of cross-linked spiral As-Se chains and their mechanical response to uniaxial stresses during fiber drawing. NQR experiments indicated that as fibers are drawn faster their NQR signal shifts to higher frequency and decreases intensity. At very rapid draw rates however distinct features resembling the sharp signals seen for crystals are observed. Both stored energy and fictive temperature measured as a function of draw rate exhibit complex behavior. This behavior can be qualitatively explained by a physical model of drawing-induced damage to, and subsequent healing of, the chain-like glass structure. The data reflect the competitive nature of both processes, where the damage mechanism includes not only inter-chain damage at lower draw rates but also intra-chain bond rupture at higher rates. Evidence of fast, low temperature relaxations has been observed in fibers drawn at the fastest rates.

VI. References

1 Stockhorst H., Bruckner R, J. Non-Cryst. Solids **49** 471 (1982)

2 Pahler G., Bruckner R, J. Non-Cryst. Solids **49** 487 (1982)

3 Stockhorst H., Bruckner R, Phys. Chem. Glasses **27** 2049 (1986)

4 Stockhorst H., Bruckner R, J. Non-Cryst. Solids **85** 105 (1986)

5 Simmons J., Mohr R.K., Monrose C.J., J. Appl. Phys. **53(6)** 4075 (1982)

6 Ho C.T., Ph.D Thesis NY State College of Ceramics, Alfred University, (1995)

7 Cerqua-Richardson K.A., Ph.D Thesis New York State College of Ceramics, Alfred University, (1992)

8 Slayter G., J. Am. Ceram Soc. **19** 335 (1936)

9 Murgatroyd J.B., J. Soc. Glass Technology **32** 291 (1948)

10 Otto W., J. Am. Ceram. Soc. **38** 122 (1955)

11 Lau J., Nakata A.M., Mackenzie J.D., J. Non-Cryst. Solids **70** 233 (1985)

12 Sheih S.H.M., LaCourse W.C., Mater. Chem. Phys.35 160 (1993)

13 Otto W., Preston F.W., J.Soc. Glass Technol.34 63 (1950)

14 Brannan R.T., J. Am. Ceram. Soc. **36**(7) 230 (1953)

15 Striling J.F., J. Soc. Glass Technol. **39** 135 (1955)

16 Otto W., J. Am. Ceram. Soc. **44** 122 (1961)

17 Sangherra J.S., Mackenzie J.D., J. Non-Cryst. Solids.125 76 (1990)

18 Banerjee B.K., J. Am. Ceram. Soc. **36** 294 (1953)

19 Goldstein M., Davies T.H., J. Am. Ceram. Soc. **38** 223 (1955)

20 Takamori T., J. Am. Ceram. Soc. **48** 170 (1965)

21 Alexander L.E., Michalik E.R., Acta Cryst. **12** 105 (1959)

22 Milberg M.E., Daly M.C., J. Chem. Phys. **39** 2966 (1963)

23 Stebbins J.F., Spearing D.R., Farnan I., J. Non-Cryst. Solids **110** (1989).

24 Chen H.S., Kurkjian C.R., J. Am. Ceram. Soc. **66** 613 (1983)

25 Moynihan C.T., Bruce A.J., Gavin D.L., Loehr S.R., Opalka S.M., Drexhage M.G., Poly. Eng. Sci.. **24** 1118 (1984)

26 Ma H.L., Zhang X.H., Lucas J., Moynihan C.T., J. Non-Cryst. Solids. **140** 209 (1992)

27 Clavaguera M., Clavaguera-Mora M.T., Surinach S., Baro M.D., J. Non-Cryst. Solids. **104** 283 (1988)

28 Sheih S.H.M., Ph.D Thesis New York State College of Ceramics, Alfred University, (1989)

29 King W.A., Clare A.G. LaCourse W.C., Volin K., Wright A.C., Sinclair R.N., Phys. Chem Glasses October (1997)

30 LaCourse W.C, Ho C.T., Cerqua-Richardson K.A., MacCrone R.K., Hari P. Taylor P.C Glasstech. Ber. Glass Sci. Technol. **68** C2 4-13 (1995)

31 Moynihan C.T., Eastel A.J., DeBolt M., Tucker J., J. Am. Ceram. Soc. **59** 12 (1976)

32 DeBolt M., Eastel A.J., Macedo P.B., Moynihan C.T.,, J. Am. Ceram. Soc. **59** 16 (1976)

33 Eastel A.J., Wilder J., Mohr R.K., Moynihan C.T., J.Am. Ceram. Soc.**60** 134 (1977)

34 Moynihan C.T., Eastel A.J., Wilder J., Tucker J., J.Phys Chem. **78** 2673 (1974)

35 Brawer S.A., *"Relaxation in Viscous Liquids and Glasses"* published by American Ceramic Society, Westerville OH, (1985)